Acta Cryst. (1992). B48, 393–400

Electron Density Study of $YBa_2Cu_3O_{6+\delta}$

BY SATOSHI SASAKI*

Photon Factory, National Laboratory for High Energy Physics, Oho, Tsukuba 305, *Japan*

AND ZENZABURO INOUE, NOBUO IYI AND SHUNJI TAKEKAWA

National Institute for Research in Inorganic Materials, Namiki, Tsukuba 305, *Japan*

(*Received* 8 *February* 1991; *accepted* 10 *January* 1992)

Abstract

Crystal structure analysis of $YBa_2Cu_3O_{6+\delta}$ was carried out using single-crystal X-ray intensity data up to $\sin\theta/\lambda = 1.22$ Å^{-1}. The crystal has a distorted perovskite structure with oxygen-deficient layers. Difference Fourier maps showed residual density around the Cu(2) atoms, which belonged to localized $3d$ electrons. A pair of residual peaks of height 3.0 e Å^{-3} are located 0.92 Å from Cu(2) along the c axis. In contrast, the Cu(1) atoms have a spherical distribution of $3d$ electrons. Atomic charges estimated by direct Fourier summations of X-ray diffraction data are +0.98 (8) and +1.78 (7) e for the Cu(1) and Cu(2) atoms, corresponding to the univalent and divalent states, respectively. The electronic configuration of the Cu(1) atoms is Cu^+, *i.e.* $3d^{10}$, having completely filled $3d$ orbitals. The configuration of the Cu(2) atoms is Cu^{2+}, *i.e.* $3d^9$, where there is one electron missing from the $3d_{x^2-y^2}$ orbitals. A positive peak of residual density, peak height 3.2 e Å^{-3}, appears 0.65 Å from the Ba atoms, along $-z$ direction. The peak still remained after treatment of anharmonic thermal vibration. A spherical distribution of electrons can be approximated around the Y atoms. Crystal data: $YBa_2(Cu_{2.898}Al_{0.102})O_{6.38}$, $M_r = 652.6$, tetragonal, $P4/mmm$, $a = 3.860$ (1), $c = 11.813$ (4) Å, $V = 176.05$ (7) Å^3, $Z = 1$, $D_x = 6.16$ Mg m^{-3}, λ(Mo $K\alpha$) = 0.7107 Å, μ(Mo $K\alpha$) = 286.7 cm^{-1}, $F(000) = 287.4$, room temperature. Final R values: (I) 0.019 ($wR = 0.019$) and (II) 0.018 (0.019) for 750 reflections averaged from 5976 measured over half a hemisphere, with $F \geq 3\sigma(F)$.

1. Introduction

Since Bednorz & Müller (1986) discovered superconductivity at 30 K in the La–Ba–Cu–O system, intensive studies have been carried out to find oxide superconductors having higher critical temperatures. So far many copper oxides having a higher T_c than liquid-nitrogen temperatures have been found in systems such as Y–Ba–Cu–O, Bi–Sr–Ca–Cu–O, Tl–Ba–Ca–Cu–O, Pb–Sr–Ca–Cu–O (Wu, Ashburn, Torng, Hor, Meng, Gao, Huang, Wang & Chu, 1987; Maeda, Tanaka, Fukutomi & Asano, 1988; Kondoh, Ando, Onoda, Sato & Akimitsu, 1988; Sheng & Hermann, 1988). From experiments such as flux quantification, magnetic flux density and the Josephson effect, pairing condensation of electrons or something similar seems to be responsible for superconductivity. However, the mechanism of high-T_c superconductivity has not yet been solved. For example, the previously reported mechanism cannot explain why superconductivity appears at high temperature and with an extremely short coherence length.

Since the discovery of high-T_c superconductors, clues as to the possible underlying mechanism of superconductivity have been provided by crystal structures and experiments concerning physical properties. Such experiments will continue to play an important part in the study of superconductivity. It is also well recognized that electronic structure, spectroscopic properties and theoretical calculations can provide important information about the strongly correlated electrons in superconductivity. High-T_c superconductors always have Cu—O layers, and therefore, it is essential to study the Cu $3d$ configurations and the presence of empty $3d$ states. $YBa_2Cu_3O_{6+\delta}$ is the most extensively studied compound related to the charge-transfer model. Two Cu atoms act as conduction and charge reservoir. The crystal structure of $YBa_2Cu_3O_{6+\delta}$ includes two crystallographically different Cu-atom sites which limit spectroscopic approaches. A local interaction in the range 10 to 50 Å is required to produce superconductivity (*e.g.* Iye, Tamegai, Takeya & Takei, 1987), suggesting interaction in the region of several unit cells. This presents a new opportunity to the crystallographer, namely to observe the electron density from accurate X-ray diffraction data. Information on the spatial distribution of electrons in the crystal

* Present address: Research Laboratory of Engineering Materials, Tokyo Institute of Technology, Nagatsuta 4259, Midori-ku, Yokohama 227, Japan.

0108-7681/92/040393-08$06.00

© 1992 International Union of Crystallography

would be particularly helpful if it were compared with binding-energy measurements, for example.

The orthorhombic–tetragonal transformation in $YBa_2Cu_3O_{6+\delta}$ ($0 \le \delta \le 1$) is known to be associated with the ordering of oxygen atoms in Cu—O chains (Sueno, Nakai, Okamura & Ono, 1987; Hewat, Capponi, Chaillout, Marezio & Hewat, 1987). The phase transformation is dependent on the temperature and partial pressure of oxygen. The orthorhombic phase which shows superconductivity around 95 K belongs to the space group *Pmmm*. The tetragonal *P4/mmm* phase is also considered to show superconductivity, at 20–40 K. The crystal structure of the twinned orthorhombic crystals was determined by the single-crystal X-ray diffraction method (Siegrist, Sunshine, Murphy, Cava & Zahurak, 1987; LePage, McKinnon, Tarascon, Greene, Hull & Hwang, 1987; Okamura, Sueno, Nakai & Ono, 1987; Sato, Nakada, Kohara & Oda, 1987; Calestani & Rizzoli, 1987). Because the orthorhombic crystals are always twinned and accurate X-ray intensity data were needed for the electron density study, a spherical crystal of the tetragonal phase was prepared for our purposes. A study in which Co or Fe atoms were substituted for Cu, suggested that the orthorhombic distortion is independent of the nature of high-T_c superconductivity (Maeno & Fujita, 1988). The impurity-induced tetragonal phase exhibits superconductivity with T_c over 80 K. In the Y–Ba–Cu–O system, the CuO_5 pyramid layer is believed to be closely related to the superconductivity, because the CuO_2 chain is absent in some types of superconductors such as Ca–La–Ba–Cu–O, Bi–Sr–Ca–Cu–O and Tl–Ba–Ca–Cu–O. Single-crystal X-ray studies on the tetragonal crystal structure have been reported by Hazen, Finger, Angel, Prewitt, Ross, Mao, Hadidiacos, Hor, Meng & Chu (1987), Nakai, Sueno, Okamura & Ono (1987), Inoue, Sasaki, Iyi & Takekawa (1987), Roth, Renker, Heger, Hervieu, Domengès & Raveau (1987), Sato, Nakada, Kohara & Oda (1988), and Garbauskas, Green, Arendt & Kasper (1988).

The partially filled 3*d* orbitals of the transition metal are affected by a strong symmetrical crystal field and they are also considered to influence the high-T_c superconductivity in oxide superconductors. Therefore, the effective atomic charges of the Cu atoms and the asphericity in the electron density distribution will be discussed in this paper. Part of this work has already been reported (Inoue, Sasaki, Iyi & Takekawa, 1987; Sasaki, Inoue, Iyi & Takekawa, 1988).

2. Experimental

Single crystals of $YBa_2Cu_3O_{6+\delta}$ were synthesized from mixed powders of $2BaO:Y_2O_3:2CuO$ (12:1:26 mole ratio). The mixture, contained in an alumina rod, was heated in an alumina crucible and melted in air at 1273 K. The melt was held at this temperature for 3 h, and then cooled at a rate of 10 K h^{-1}, before being poured out of the crucible at 1153 K. Many single crystals were found on the surface of the alumina rod. The shape of the crystal was rectangular and the maximum length was about 0.5 mm. Only a single phase of $YBa_2Cu_3O_{6+\delta}$ could be detected in the electron probe microanalyser (EPMA) and polarized microscope analysis. Single crystals $0.2 \times 0.2 \times 0.2$ mm were chosen for the X-ray determination of the space group. A single crystal was ground into a sphere of 0.12 mm in diameter and used for crystal structure analyses. The symmetry of this phase was confirmed by the X-ray precession method using a four-circle diffractometer. The intensity distribution indicated tetragonal symmetry with Laue group 4/*mmm*. No split peaks due to Bragg reflections were observed. Because no systematic absences were observed, possible space groups are $P\bar{4}2m$, $P\bar{4}m2$, *P*422, *P*4*mm* and *P*4/*mmm*. Difference Fourier maps using reflections observed within a hemisphere show that the distribution of difference electron density is consistent with that derived from the space group D^1_{4h}–*P*4/*mmm*. Cell dimensions were calculated by the least-squares method using 2θ values of 50 reflections ($53.3 \le 2\theta \le 73.0°$) measured with a Rigaku AFC-5 four-circle diffractometer (Mo $K\alpha_1$ radiation; $\lambda = 0.70926$ Å). The unit-cell values are $a = 3.860\,(1)$ and $c = 11.813\,(4)$ Å.

Integrated intensity data up to $2\theta = 120°$ were collected using Mo $K\alpha$ radiation ($\lambda = 0.7107$ Å) monochromatized by graphite (002). The ω–2θ scan mode of the four-circle diffractometer was used with a scan speed of 2° min^{-1} and a scan width of $(1.2 + \tan\theta)°$ in ω. Three standard reflections were stable within ±0.8% of integrated intensity during the data collection. The minimum and maximum intensities are 40 267 and 41 474 for the 220 reflection, 40 364 and 42 911 for $\bar{2}20$, and 40 418 and 42 405 for $2\bar{2}0$. The range of *hkl* values measured was $-9 \le h \le 9$, $-9 \le k \le 9$ and $0 \le l \le 28$. Of a total of 5976 measured reflections, 750 and 4510 reflections with $F \ge 3\sigma(F)$ were used for refinement after averaging all equivalent reflections ($R_{int} = 0.024$) and for refinement assuming lower symmetry, respectively. The Patterson, Fourier and difference Fourier methods were used to solve the crystal structure (*FRAXY*; Sasaki, 1987).

After corrections for Lorentz and polarization effects and spherical absorption, all parameters (scale factor, extinction parameter, atomic coordinates and temperature factors) were refined simultaneously using the full-matrix least-squares program *RADY* (Sasaki, 1987), which is a revised version of *ORFLS*

(Busing, Martin & Levy, 1963). Residuals of the function $\sum w_i(|F_o| - |F_c|)^2$ were minimized with $w_i = 1/\sigma^2(F)$. An isotropic extinction correction was applied following Becker & Coppens (1974). No anisotropic correction was applied because (*a*) reasonable results were obtained using the isotropic model and (*b*) a small number of assumed models (fewer parameters refined) is preferable in order to prevent misinterpreting residual electron density. Information concerning the least-squares refinements is listed in Table 1. Final R and wR values for the refinement with anisotropic temperature factors were 0.019 and 0.020, respectively. Atomic scattering factors for Y^{3+}, Ba^{2+}, Cu^{2+} and Al^{3+} were taken from *International Tables for X-ray Crystallography* (1974, Vol. IV) and that for O^{2-} was from Tokonami (1965). The atomic scattering factors provide a reference model in difference Fourier syntheses. They are based on the total wavefunctions obtained by the modified Dirac–Slater method (Y^{3+} and Ba^{2+}), the +1 well-potential model (O^{2-}) and the relativistic Hartree–Fock method (all other atoms). Anomalous-scattering factors were also taken from *International Tables for X-ray Crystallography* (1974, Vol. IV). The transmission factors ranged from 0.096 to 0.177. The result of the structure refinement using 750 reflections is given in Table 2 which includes site-occupancy parameters, atomic coordinates and temperature factors.* Difference Fourier maps synthesized after final refinement showed minimum and maximum residual densities of ± 3.0 e Å^{-3}. The refinement with 4510 reflections within a hemisphere gives $R = 0.029$ and $wR = 0.030$ (goodness of fit, $S = 2.04$) with the maximum $\Delta/\sigma = 0.0032$ (z of Ba).

3. Crystal structure

The structure of $YBa_2Cu_3O_{6+\delta}$ can be described as an oxygen-defect perovskite. Oxygen atoms located at $z = \frac{1}{2}$ are fully removed from the ideal ABO_3 stoichiometry (Y and Ba in A and Cu in B). The Y and Ba atoms have cubic eightfold and distorted 12-fold coordinations, respectively. The crystal structure is shown in Fig. 1. The stacking along the c axis is in a [Ba—Y—Ba] with Ba—Ba and Ba—Y bond distances of 4.593 (1) and 3.610 (1) Å, respectively. The Y—O(3) distance is 2.400 (1) Å, while the Ba—O distances vary from 2.772 (1) to 3.000 (1) Å. Bond distances for Cu atoms are Cu(1)—O(1) = 1.809 (1), Cu(1)—O(2) = 1.930 (1), Cu(2)—O(3) = 1.942 (1) and Cu(2)—O(1) = 2.453 (1) Å.

* Lists of structure factors have been deposited with the British Library Document Supply Centre as Supplementary Publication No. SUP 54899 (15 pp.). Copies may be obtained through The Technical Editor, International Union of Crystallography, 5 Abbey Square, Chester CH1 2HU, England. [CIF reference: OH0012]

Table 1. *Experimental data for* $YBa_2Cu_3O_{6+\delta}$

(I) Refinement with anisotropic temperature factors, (II) refinement with anharmonic thermal parameters for the Ba atom. $wR = [\sum w(|F_o| - |F_c|)^2 / \sum wF_o^2]^{1/2}$; $S = [\sum w(|F_o| - |F_c|)^2/(m-n)]^{1/2}$.

	(I)	(II)
Maximum 2θ (°)	120	120
No. of reflections		
Observed	5976	5976
Refined	4510	4510
Refined (independent)	750	750
No. of parameters refined	27	32
R	0.019	0.018
wR	0.019	0.019
S	1.16	1.11
Extinction g ($\times 10^{-4}$)	0.416 (3)	0.410 (3)
$(\Delta\sigma)$ for z of Ba	0.0029	0.0030
$(\Delta\sigma)$ for z of Cu(2)	0.0026	0.0042
$(\Delta\sigma)_{max}$	0.0029	0.0042
$(\Delta\rho)_{max}$ (e Å^{-3})	3.0	3.2
$(\Delta\rho)_{min}$ (e Å^{-3})	−3.0	1.8

Refining the site multiplicity shows that the site occupancy of the Cu and O atoms in the Cu(1) and O(2) sites is 0.933 (2) and 0.19 (1), respectively. The deficiency of Cu atoms in Cu(1) sites can be explained by the existence of Al atoms in the sites. This is because the crystal grown was possibly contaminated with Al from the alumina rod and crucible. Therefore, a final site-occupancy refinement was carried out assuming that Cu and Al atoms share the Cu(1) sites. The result shows that the proportion of Al to Cu is in the ratio 0.102 to 0.898 (3). The other sites such as Y, Ba, Cu(2), O(1) and O(3) are fully occupied by the respective atoms. Thus, the chemical formula based on the refinement can be written as $YBa_2(Cu_{2.898}Al_{0.102})O_{6+\delta}$ ($\delta = 0.38$). The crystal used here lies close to the tetragonal–orthorhombic phase boundary in view of the δ value, which illustrates the oxygen deficiency. Oxygen atoms occupy 19% of the O(2) sites. In a stoichiometric tetragonal crystal ($\delta = 0$), the O(2) sites are perfectly vacant (Onoda,

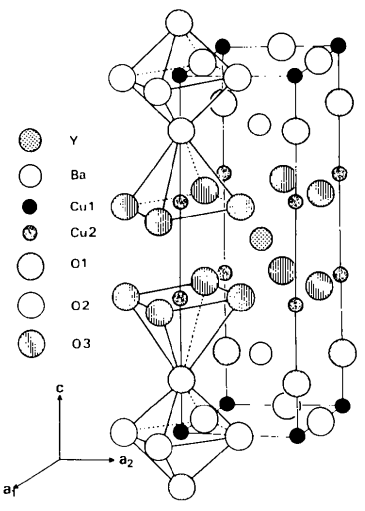

Fig. 1. Crystal structure of tetragonal $YBa_2Cu_3O_{6+\delta}$. Two different kinds of Cu site are represented by oxygen polyhedra.

Table 2. *Site occupancy, atomic coordinates and thermal parameters of* $YBa_2Cu_3O_{6.38}$

The β_{ij}'s are defined by $\exp[-(h^2\beta_{11} + k^2\beta_{22} + l^2\beta_{33} + 2hk\beta_{12} + 2hl\beta_{13} + 2kl\beta_{23})]$. For each atom the second row gives the result of the refinement with anharmonic thermal parameters for the Ba atom.

		Occupancy*	x	y	z	β_{11}	β_{22}	β_{33}	B_{eq}†
Y		1.0014	$\frac{1}{2}$	$\frac{1}{2}$	$\frac{1}{2}$	0.00511 (6)	$=\beta_{11}$	0.000978 (1)	0.385 (1)
						0.00512 (6)		0.000948 (1)	0.380 (1)
Ba		1.9986 (8)	$\frac{1}{2}$	$\frac{1}{2}$	0.194390 (8)	0.00995 (3)	$=\beta_{11}$	0.001250 (1)	0.628 (1)
					0.19418 (1)	0.00983 (7)		0.001168 (1)	0.608 (2)
Cu(1)	Cu	0.898 (3)	0	0	0	0.0155 (1)	$=\beta_{11}$	0.001125 (2)	0.824 (3)
	Al	0.102							
						0.0153 (1)		0.001118 (2)	0.816 (3)
Cu(2)		2.000 (2)	0	0	0.36085 (2)	0.00390 (5)	$=\beta_{11}$	0.001444 (1)	0.424 (1)
					0.36086 (2)	0.00386 (5)		0.001423 (1)	0.418 (1)
O(1)		2	0	0	0.1531 (1)	0.0223 (6)	$=\beta_{11}$	0.001506 (8)	1.17 (1)
					0.1531 (1)	0.0219 (5)		0.001475 (8)	1.15 (1)
O(2)		0.38 (1)	0	$\frac{1}{2}$	0	0.63 (9)	0.13 (4)	0.0104 (4)	17 (3)
						0.60 (8)	0.17 (4)	0.0069 (3)	16 (2)
O(3)		4	$\frac{1}{2}$	0	0.37921 (7)	0.0031 (3)	0.0075 (4)	0.001765 (5)	0.54 (1)
					0.37916 (7)	0.0031 (3)	0.0074 (3)	0.001764 (5)	0.54 (1)

* Multiplicities of Y, Ba, Cu(2) and O(2) sites were refined using the atomic scattering factors of the constituent atoms.
† Equivalent isotropic temperature factors (Hamilton, 1959).

Shamoto, Sato & Hosoya, 1987). The charge deviation from neutrality was estimated to be -0.54 e from the chemical formula.

The Cu(2) atom is coordinated to five oxygen atoms, where the oxygen atoms form a square plane and a pyramid apex. The pyramid polyhedra form layers perpendicular to the c axis. The Cu—O distances to the oxygen in the plane and to the pyramid apex are 1.942 (1) and 2.453 (1) Å, respectively. The distance from the Cu(2) atom to the O(3) square plane is 0.217 Å. On the other hand, the Cu(1) octahedron has two short (1.809 Å) and four long (1.930 Å) Cu—O bonds. Because the oxygen atoms of the longer bond are only 19% occupied, the Cu(1) atom is approximated as being coordinated to two oxygen atoms and having the stacking sequence [O(1)—Cu(1)—O(1)] along the c axis.

4. Electron density distribution

The difference Fourier maps of $YBa_2Cu_3O_{6+\delta}$ were synthesized using the $|F_o| - |F_c|$ values obtained in the final step of the refinement. Atomic scattering factors used for the F_c calculation are assumed to be spherically symmetric in the electron density of the atoms. In these maps the highest positive peaks appear around the Ba and Cu(2) atoms with peak heights of 3.0 e Å^{-3}. The lowest negative peaks are -3.0 e Å^{-3} around Ba atoms. Strict assessment of the significance of the difference electron density is very difficult but the reliability may be estimated from statistical tests in the least-squares refinement such as the goodness-of-fit (see Table 1). In practice, a significant error may roughly be estimated as ± 0.5 e Å^{-3} from the values of most spurious residual densities.

The difference Fourier map for the section $x_1 = 0$ is shown in Fig. 2(*a*). No residual electron density was observed around Cu(1) atoms, showing a spherical distribution of 3*d* electrons. In contrast, asphericity of the electron distribution was clearly observed around the Cu(2) atom. The residual density peak of localized *d* electrons appears with a peak height of 3.0 e Å^{-3} at 0.92 Å from the Cu(2) atom along the c axis. One of the residual peaks closer to $z = \frac{1}{2}$ is linked with its partner which is related by mirror symmetry on (001) at $z = \frac{1}{2}$. The distance between the two peaks with mirror symmetry is 1.43 Å. The relationship between residual peaks and the neighboring atoms is shown schematically in Fig. 3. Since the distance between the center of the Cu atom and the residual peaks is close to the radius of the 3*d* orbitals, the asphericity around the Cu(2) atom can be considered to arise from the configuration of the 3*d* electrons. A difference Fourier map perpendicular to the c axis and passing through the Cu(2) site is also shown in Fig. 4. No unusual residual density peaks were observed in the a_1a_2 plane. There may be slightly positive areas between the Cu(2) and O(3) bonds and slightly negative areas off the bonds. The possible electronic structures will be discussed later. There are some reports on the residual electron density of copper compounds (Tanaka, Konishi & Marumo, 1979; Varghese & Maslen, 1985; Restori & Schwarzenbach, 1986).

Fig. 2(*b*) shows the (010) section of the difference Fourier map at $x_1 = 0.5$ where Y, Ba, and O(3) atoms are included on the plane. No unusual residual peaks appear around the Y atom. There might be four positive and two (or ten) negative peaks, but the residual density is not significantly greater than the background levels. The approximately spherical electron distribution suggests completely filled Y^{3+} 4*s*4*p* orbitals. Two positive peaks were found around the Ba atoms. One peak with the height of 2.4 e Å^{-3} is away from (0.13 Å) the Ba atom, which is associated with a negative peak of -1.2 e Å^{-3}. The characteristic pattern suggests the presence of anharmonic thermal motion: the residual peaks are the result of misfitting of the thermal model. The second positive

peak appears at a distance of 0.63 Å from the Ba atom, and has a height of 3.0 e Å^{-3}. The electron density distribution around the Ba atom will be discussed after further discussion of thermal vibration.

5. Anharmonic thermal vibration of the Ba atoms

Observation of the difference Fourier maps suggests that anharmonic terms for the thermal vibration of the Ba atoms should be included in the refinement procedure. In order to distinguish the aspherical electron distribution from the thermal vibration effect, high-order tensors for the temperature factor are taken into account. The Gram–Charlier expansion is used to represent the Gaussian probability density function according to §5 of *International Tables for X-ray Crystallography* (1974, Vol. IV). Then, the crystal structure factor is represented as

$$F(\mathbf{h}) = \sum f \exp(2\pi i \mathbf{h}.\mathbf{x}) t(\mathbf{h}). \quad (1)$$

The Debye–Waller factor $t(\mathbf{h})$ is then given by

$$t(\mathbf{h}) = [1 + (3!)^{-1}(2\pi i)^3 c_{pqr} h_p h_q h_r + (4!)^{-1}(2\pi i)^4 d_{pqrs} h_p h_q h_r h_s + \ldots]\exp(-\beta_{pq} h_p h_q), \quad (2)$$

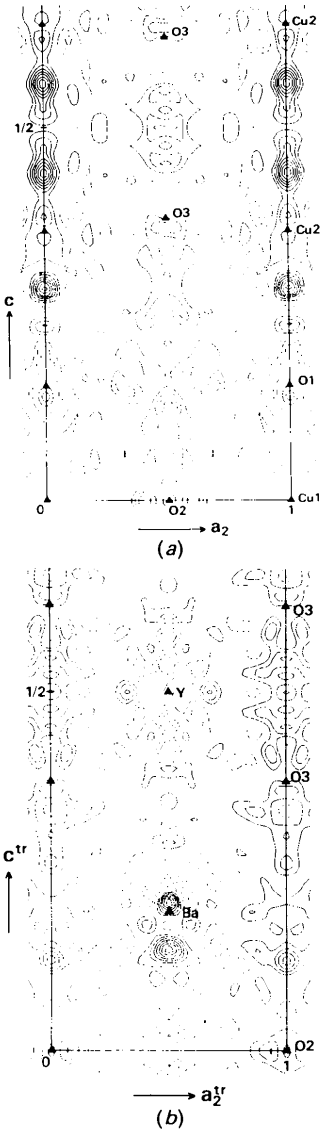

Fig. 2. Difference Fourier maps of the complete refinement using anisotropic temperature factors. (*a*) $z = 0$, (*b*) $z = 0.5$. Contour lines are drawn at intervals of 0.4 e Å^{-3}. Contours in negative regions are dashed; zero contour is omitted.

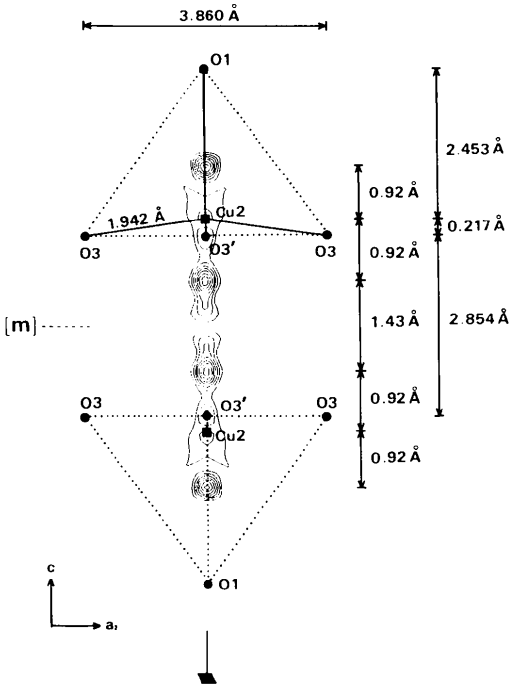

Fig. 3. Schematic diagram of residual electron density around Cu(2)—O pyramids in $YBa_2Cu_3O_{6-\delta}$. Residual peaks in Fig. 2 and neighboring atoms are given with distances.

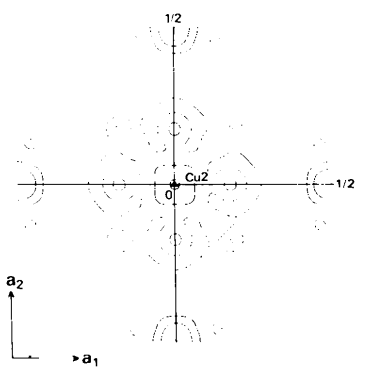

Fig. 4. A difference Fourier map passing through the Cu(2) atom at $z = 0.36085$. Contours are as in Fig. 2.

where **h** are the Miller indices and β is the anisotropic temperature factor. Tensors up to the fourth rank were used in the least-squares refinement. The anharmonic parameters for the Ba atom were refined simultaneously with other atomic parameters. The values (multiplied by 10^6) are as follows: $c_{113} = c_{233} = -1.12$ (7), $c_{333} = -0.072$ (7), $d_{1111} = d_{2222} = -0.02$ (2), $d_{1133} = d_{2233} = -0.020$ (4) and $d_{3333} = -0.0025$ (3). The other atomic parameters are listed in Table 2. The values of z and β_{33} for the Ba atom changed significantly when thermal vibration was treated anharmonically. The Ba position shifted 0.0025 Å in the $-z$ direction and β_{33} became 7% smaller. The temperature factor β_{11} did not change significantly ($\sim 1\%$). Anharmonic parameters for the Cu atoms were not introduced in the final refinement because of the small change in the residual density distribution around Cu(2) atoms and in order to prevent overestimation of the thermal vibration.

The (100) difference Fourier maps were synthesized using the same conditions as before, *i.e.* using structure factors calculated from the anharmonic model (Fig. 5). Only one positive peak remains at a distance of 0.65 Å from the center of the Ba atom, in the $-z$ direction. The peak is high (3.2 e Å^{-3}). Generally, a spherical distribution is expected for the Ba atom, because the 5*s*5*p* orbitals are completely filled in the divalent state. Therefore, a question remained regarding the crystal structure. The residual electron density is located towards a vacancy in the Cu(1)—O net plane where the O(2) sites are deficient in O atoms. A small number of Ba atoms may modulate slightly towards the vacancy depending on whether O atoms exist in the O(2) sites or not.

6. Atomic charges of the Cu atoms

Here atomic charge is defined as the number of electrons belonging to a specific atom. The number of electrons within a sphere of radius R around an atom can be expressed as

$$\begin{aligned} C(R) &= \int \rho(r)\mathrm{d}V \\ &= \int_{r<R} V^{-1}[\textstyle\sum\sum\sum_{h\ k\ l} F(hkl)\exp(-2\pi i\mathbf{s}.\mathbf{r})]\mathrm{d}V \\ &= V^{-1}\{4\pi R^3 F(000)/3 + (2\pi^2)^{-1} \\ &\quad \times \textstyle\sum\sum\sum' [s^{-3}F(hkl)\exp(-2\pi i\mathbf{s}.\mathbf{r}) \\ &\quad \times (-2\pi sR\cos 2\pi sR + \sin 2\pi sR)]\}, \end{aligned} \tag{3}$$

where $\rho(r)$ is the electron density at a point r in a unit cell; $\mathbf{s} = h\mathbf{a}^* + k\mathbf{b}^* + l\mathbf{c}^*$ and $s = |\mathbf{s}| = 2\sin\theta/\lambda$ (Sasaki, Fujino, Takéuchi & Sadanaga, 1980). The $F(hkl)$'s calculated from atomic parameters were applied to 1000 unobserved reflections within the observation sphere. The termination effect of Fourier series outside the observation sphere was corrected by the Romberg method of numerical integration. After calculation of $C(R)$ at intervals of 0.01 Å, the radial distribution function $U(R)$ was obtained by differentiating $C(R)$ with respect to R. Cu atoms can be separated from neighboring O atoms by a minimum value of $U(R)$.

$U(R)$'s for two kinds of Cu atom are shown in Fig. 6. The deficiency in Cu(1) sites was normalized to the fully occupied state by multiplying the reverse of the occupancy parameter. The first $U(R)$ peaks are Cu atoms, while the second peaks near 2 Å are the neighboring O atoms. A low electron density region exists between the Cu and O atoms, where a $U(R)$ minimum is clearly visible (Table 3). When the

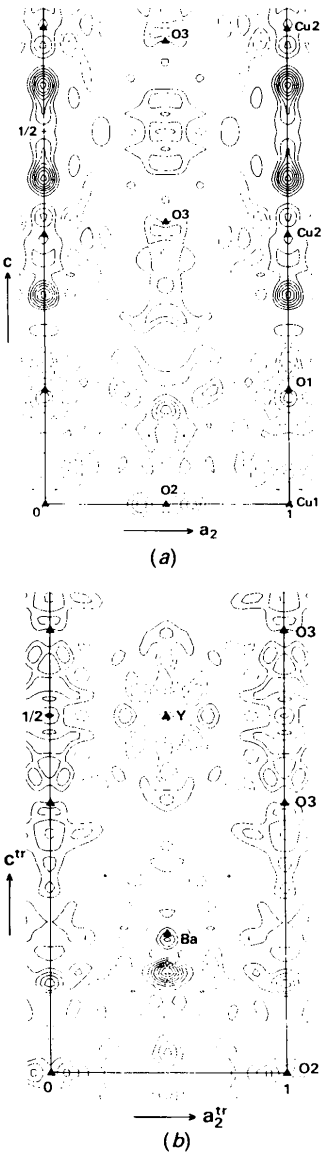

Fig. 5. Difference Fourier maps on (100) based on the refinement using anharmonic thermal parameters for Ba atoms. (*a*) $z = 0$, (*b*) $z = 0.5$. Contours are as in Fig. 2.

Table 3. *Atomic radius, number of electrons, C(R), and radial distribution functions, U(R), for* Cu *atoms of* $YBa_2Cu_3O_{6+\delta}$

Values in parentheses represent the estimated errors of $C(R)$ based on $\sigma F(hkl)$. Formal charges corresponding to the radius and $U(R)$ are given in the 'Charge' column. EDR is defined as a $U(R)$ minimum between Cu and O atoms.

	Cu(1)				Cu(2)		
Radius (Å)	$U(R)$ (e Å^{-1})	$C(R)$ (e)	$C_n(R)$ (e)	Charge	$U(R)$ (e Å^{-1})	$C(R)$ (e)	Charge
0.60	18.33	22.12 (4)	23.71		19.97	24.06 (4)	
0.62	16.69	22.50 (4)	24.12		18.27	24.45 (4)	
0.64	15.16	22.85 (4)	24.49		16.60	24.80 (4)	
0.66	13.75	23.17 (4)	24.83		14.98	25.11 (4)	+4
0.68	12.47	23.46 (4)	25.14	+4	13.44	25.38 (4)	
0.70	11.30	23.72 (5)	25.42		11.97	25.61 (5)	
0.72	10.25	23.94 (5)	25.66		10.61	25.80 (5)	
0.74	9.31	24.14 (5)	25.87		9.36	25.96 (5)	+3
0.76	8.48	24.31 (5)	26.06	+3	8.22	26.09 (5)	
0.78	7.75	24.45 (5)	26.21		7.20	26.20 (5)	
0.80	7.12	24.57 (5)	26.33		6.31	26.29 (5)	
0.82	6.57	24.66 (5)	26.43		5.53	26.37 (5)	
0.84	6.10	24.73 (6)	26.51		4.87	26.44 (6)	
0.86	5.70	24.80 (6)	26.58		4.33	26.51 (6)	
0.88	5.36	24.85 (6)	26.63		3.88	26.59 (6)	
0.90	5.08	24.91 (6)	26.70		3.53	26.68 (6)	
0.92	4.83	24.98 (6)	26.77		3.26	26.78 (6)	
0.94	4.62	25.04 (6)	26.84		3.07	26.88 (6)	
0.96	4.44	25.12 (7)	26.92		2.95	26.99 (7)	+2
0.98	4.28	25.20 (7)	27.01	+2	2.87	27.10 (7)	
1.00	4.15	25.30 (7)	27.12		2.85	27.22 (7)	EDR
1.02	4.03	25.42 (7)	27.25		2.87	27.32 (7)	
1.04	3.92	25.54 (7)	27.37		2.92	27.42 (7)	
1.06	3.83	25.67 (8)	27.51		3.00	27.50 (8)	
1.08	3.76	25.80 (8)	27.65		3.11	27.57 (8)	
1.10	3.70	25.94 (8)	27.80		3.24	27.62 (8)	
1.12	3.66	26.07 (8)	27.94	+1	3.40	27.66 (8)	
1.14	3.65	26.18 (8)	28.06	EDR	3.60	27.68 (8)	
1.16	3.67	26.29 (8)	28.18		3.82	27.72 (8)	
1.18	3.72	26.38 (9)	28.27		4.07	27.74 (9)	
1.20	3.81	26.45 (9)	28.35		4.36	27.77 (9)	
1.22	3.94	26.50 (9)	28.40		4.69	27.80 (9)	
1.24	4.13	26.55 (9)	28.46		5.06	27.85 (9)	
1.26	4.37	26.58 (9)	28.49		5.48	27.93 (9)	
1.28	4.67	26.61 (9)	28.52		5.93	28.03 (9)	+1
1.30	5.03	26.65 (9)	28.56		6.43	28.15 (9)	
1.32	5.46	26.70 (10)	28.62		6.97	28.31 (10)	
1.34	5.95	26.77 (10)	28.69		7.54	28.50 (10)	
1.36	6.51	26.86 (10)	28.79		8.15	28.71 (10)	
1.38	7.13	26.98 (10)	28.92		8.78	28.94 (10)	0
1.40	7.81	27.13 (10)	29.08	0	9.43	29.19 (10)	
1.42	8.55	27.32 (10)	29.28		10.09	29.45 (10)	
1.44	9.35	27.54 (10)	29.52		10.75	29.71 (10)	
1.46	10.19	27.79 (10)	29.79		11.42	29.97 (10)	
1.48	11.09	28.06 (11)	30.08		12.09	30.23 (11)	
1.50	12.02	28.35 (11)	30.39		12.75	30.48 (11)	
1.52	13.00	28.66 (11)	30.72		13.43	30.72 (11)	
1.54	14.01	28.97 (11)	31.05		14.13	30.96 (11)	
1.56	15.06	29.30 (11)	31.40		14.86	31.21 (11)	
1.58	16.15	29.63 (11)	31.76		15.66	31.46 (11)	
1.60	17.28	29.96 (11)	32.11		16.57	31.73 (11)	

effective distribution radius EDR is defined as the distance from an atom to the $U(R)$ minimum (Sasaki, Fujino, Takéuchi & Sadanaga, 1980), the EDR values are 1.14 and 1.00 Å for the Cu(1) and Cu(2) atoms, respectively. By counting the number of electrons within the EDR, atomic charges for Cu(1) and Cu(2) atoms were obtained as +0.98 (8) and +1.78 (7) e, respectively. Ambiguity in determining the EDR was estimated from the relationship between $U(R)$ and R for various formal charges (Table 3). After consideration of the EDR ambiguity, it is concluded that the Cu(1) and Cu(2) sites are occupied by Cu^+ and Cu^{2+} ions, respectively. From the values of $U(R)$ in Table 3 it can be seen that radii corresponding to divalent copper for Cu(1) and trivalent copper for Cu(2) still remain within shoulders of the first peaks of Cu atoms, while radii of neutral Cu(1) and univalent Cu(2) are within peak shoulders of the neighboring O atoms.

In tetragonal $YBa_2Cu_3O_6$, the oxygen atoms in O(2) sites are perfectly vacant and the Cu(1) atom coordinates to two O(3) atoms. The crystallographic data of well known copper compounds suggest that the formal charge of copper coordinated on opposite sides by two oxygen atoms is univalent. Cu^+ in Cu_2O (cuprite) is a typical example. Divalent copper for the Cu(2) site of $YBa_2Cu_3O_6$ can be derived directly from the chemical formula and charge neutrality assuming ions such as Y^{3+}, Ba^{2+} and O^{2-}. This is also consistent with Cu^+ on Cu(1) sites. Thus, the crystal structural aspect also supports the electron counting result.

7. Electronic structure

The estimated atomic charges for the Cu atoms agree with the characteristics of the electron density distribution observed on difference Fourier maps. Electrons of the Cu atoms in Cu(1) sites are distributed spherically. An atomic charge of +0.98 (8) e for Cu(1) suggests a univalent oxidation state with the $3d^{10}$ configuration where the $3d$ orbitals are fully occupied by electrons. In contrast, the electron density study around Cu(2) atoms revealed the presence of unoccupied $3d$ electron orbitals. An estimation of the atomic charge for the Cu(2) site suggests a divalent ionic state Cu^{2+} resulting from the $3d^9$ configuration.

Positive residual peaks around the Cu(2) sites appear perpendicular to the basal plane of CuO_4.

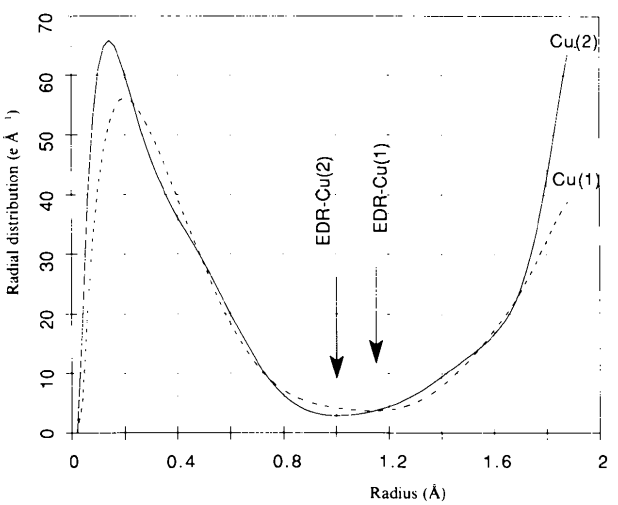

Fig. 6. Radial electron distributions in Cu(1) and Cu(2) polyhedra of $YBa_2Cu_3O_{6+\delta}$. The radius EDR is defined by a minimum position between two humps of each $U(R)$ curve.

Two residual peaks appear: one of which is in the direction of the pyramid apex, and the other is in the opposite direction. A pair of positive peaks appear to be centric around the Cu(2) site although the site does not have the point symmetry of a center. The electron distribution is consistent with a field in which the $3d$ orbitals have a center of symmetry. The site symmetry of the Cu(2) sites, therefore, is approximately D_{4h}. This ligand-field splitting may have important consequences for the nature of the $3d$ orbital bonding. The energy level of Cu^{2+} $3d^9$ is split into e_g and t_{2g} states in the octahedral field (O_h). In the tetragonal D_{4h} field, the e_g state is split into a_{1g} and b_{1g}, while the t_{2g} state is split into e_g and b_{2g}. The a_{1g} state is occupied by an electron and the other states are completely filled. Here, the a_{1g} and b_{1g} levels correspond to $3d_{x^2-y^2}$ and $3d_{z^2}$ orbitals, respectively. In the distribution of residual electron densities, a pair of positive peaks corresponds to $3d_{z^2}$ orbitals (Fig. 3) and there are no remarkable peaks in the plane of the $3d_{x^2-y^2}$ orbitals (Fig. 4). Thus, this suggests that a $3d_{x^2-y^2}$ orbital remains unoccupied. There is one hole in the unoccupied $3d_{x^2-y^2}$ orbital which may be considered as a charge carrier.

The importance for high-T_c superconductivity lies in evaluating the effect of electron overlap between Cu and O atoms. One possibility is that a Fermi surface arises from a strong hybridization of copper and oxygen orbitals. In this case Cu $3d$ orbitals overlap with $2p$ orbitals of neighboring oxygen atoms, and the configuration of O $2p_\sigma$ + Cu $3d_{x^2-y^2}$ is expected. On the other hand, if strong chemical bonding exists with Cu and O orbitals deeply below the Fermi level, d and p orbitals cannot be treated separately. The latter suggests the occurrence of residual density at the positions of the hybridized orbitals in the state of the nonsuperconducting oxide above T_c. Furthermore, in an electron distribution the characteristic is probably preserved in the room-temperature measurement. It is, however, inconsistent with our result (Fig. 4). In the former instance there is a possibility that the electron distribution changes around T_c. Since the coherent mobile object in superconductivity is an electron, the difference in the electron density between superconductive and nonsuperconductive states may be cited. Thus, an electron density study at a temperature lower than T_c is needed.

We thank Dr N. Haga of Himeji Institute of Technology for the treatment of anharmonic thermal parameters. All computations were carried out on FACOM M360 MP and M780/10R computers at the Computer Center of the Photon Factory.

References

BECKER, P. J. & COPPENS, P. (1974). *Acta Cryst.* **A30**, 129–147.

BEDNORZ, J. G. & MÜLLER, K. A. (1986). *Z. Phys. B*, **64**, 189–193.

BUSING, W. R., MARTIN, K. O. & LEVY, H. A. (1963). *ORFLS*. Report ORNL-TM-305. Oak Ridge National Laboratory, USA.

CALESTANI, G. & RIZZOLI, C. (1987). *Nature (London)*, **328**, 606–607.

GARBAUSKAS, M. F., GREEN, R. W., ARENDT, R. H. & KASPER, J. S. (1988). *Inorg. Chem.* **27**, 871–873.

HAMILTON, W. C. (1959). *Acta Cryst.* **12**, 609–610.

HAZEN, R. M., FINGER, L. W., ANGEL, R. J., PREWITT, C. T., ROSS, N. L., MAO, H. K., HADIDIACOS, C. G., HOR, P. H., MENG, R. L. & CHU, C. W. (1987). *Phys. Rev. B*, **35**, 7238–7241.

HEWAT, A. W., CAPPONI, J. J., CHAILLOUT, C., MAREZIO, M. & HEWAT, E. A. (1987). *Solid State Commun.* **64**, 301–307.

INOUE, Z., SASAKI, S., IYI, N. & TAKEKAWA, S. (1987). *Jpn. J. Appl. Phys.* **26**, L1365–L1367.

IYE, Y., TAMEGAI, T., TAKEYA, H. & TAKEI, H. (1987). *Jpn. J. Appl. Phys.* **26**, L1057–L1059.

KONDOH, S., ANDO, Y., ONODA, M., SATO, M. & AKIMITSU, J. (1988). *Solid State Commun.* **65**, 1329–1331.

LEPAGE, Y., MCKINNON, W. R., TARASCON, J. M., GREENE, L. H., HULL, G. W. & HWANG, D. M. (1987). *Phys. Rev. B*, **35**, 7245–7248.

MAEDA, H., TANAKA, Y., FUKUTOMI, M. & ASANO, T. (1988). *Jpn. J. Appl. Phys.* **27**, L209–L210.

MAENO, Y. & FUJITA, T. (1988). *Physica*, **C153–155**, 1105–1110.

NAKAI, I., SUENO, S., OKAMURA, F. P. & ONO, A. (1987). *Jpn. J. Appl. Phys.* **26**, L788–L790.

OKAMURA, F. P., SUENO, S., NAKAI, I. & ONO, A. (1987). *Mater. Res. Bull.* **22**, 1081–1085.

ONODA, M., SHAMOTO, S., SATO, M. & HOSOYA, S. (1987). *Jpn. J. Appl. Phys.* **26**, L876–L878.

RESTORI, R. & SCHWARZENBACH, D. (1986). *Acta Cryst.* **B42**, 201–208.

ROTH, G., RENKER, B., HEGER, G., HERVIEU, M., DOMENGÈS, B. & RAVEAU, B. (1987). *Z. Phys. B*, **69**, 53–59.

SASAKI, S. (1987). *RADY*. KEK Internal Report 87-3. National Laboratory for High Energy Physics, Japan.

SASAKI, S., FUJINO, K., TAKÉUCHI, Y. & SADANAGA, R. (1980). *Acta Cryst.* **A36**, 904–915.

SASAKI, S., INOUE, Z., IYI, N. & TAKEKAWA, S. (1988). *Jpn. J. Appl. Phys.* **27**, L206–L208.

SATO, S., NAKADA, I., KOHARA, T. & ODA, Y. (1987). *Jpn. J. Appl. Phys.* **26**, L663–L664.

SATO, S., NAKADA, I., KOHARA, T. & ODA, Y. (1988). *Acta Cryst.* **C44**, 11–14.

SHENG, Z. Z. & HERMANN, A. M. (1988). *Nature (London)*, **332**, 55–58.

SIEGRIST, T., SUNSHINE, S., MURPHY, D. W., CAVA, R. J. & ZAHURAK, S. M. (1987). *Phys. Rev. B*, **35**, 7137–7139.

SUENO, S., NAKAI, I., OKAMURA, F. P. & ONO A. (1987). *Jpn. J. Appl. Phys.* **26**, L842–L844.

TANAKA, K., KONISHI, M. & MARUMO, F. (1979). *Acta Cryst.* **B35**, 1303–1308.

TOKONAMI, M. (1965). *Acta Cryst.* **19**, 486.

VARGHESE, J. N. & MASLEN, E. N. (1985). *Acta Cryst.* **B41**, 184–190.

WU, M. K., ASHBURN, J. R., TORNG, C. J., HOR, P. H., MENG, R. L., GAO, L., HUANG, Z. J., WANG, Y. Q. & CHU, C. W. (1987). *Phys. Rev. Lett.* **58**, 908–910.